ISSN 1063-7761, Journal of Experimental and Theoretical Physics, 2013, Vol. 117, No. 4, pp. 691–698. © Pleiades Publishing, Inc., 2013.

ORDER, DISORDER, AND PHASE TRANSITION IN CONDENSED SYSTEM

The Influence of Defects on Magnetic Properties of fcc-Pu[1]

A. O. Shorikov[a,b], V. I. Anisimov[a,b], M. A. Korotin[a], V. V. Dremov[c], and Ph. A. Sapozhnikov[c]

[a] *Institute of Metal Physics, Russian Academy of Sciences, Yekaterinburg, 620990 Russia*

[b] *Theoretical Physics and Applied Mathematic Department, Ural State Technical University Yekaterinburg, 620002 Russia*

[c] *Russian Federal Nuclear Center "Institute of Technical Physics," Snezhinsk, Chelyabinsk oblast, 456770 Russia*

e-mail: vvd0531@mail.ru

Received February 6, 2013

Abstract—The influence of vacancies and interstitial atoms on magnetism in Pu is considered in the framework of the density functional theory. The crystal structure relaxation arising due to various types of defects is calculated using the molecular dynamics method with a modified embedded atom model. The local density approximation with explicit inclusion of Coulomb and spin–orbit interactions is applied in matrix invariant form to describe correlation effects in Pu with these types of defects. The calculations show that both vacancies and interstitials give rise to local moments in the *f*-shell of Pu in good agreement with experimental data for aged Pu. Magnetism appears due to the destruction of a delicate balance between spin–orbit and exchange interactions.

DOI: 10.1134/S1063776113120091

1. INTRODUCTION

Band structure calculations of δ-Pu predict the static magnetic order of *f*-electrons with the full magnetic moment values 0.25–5 μ_B with a substantial impact of the spin moment [1–4]. These results contradict the experimental measurements of magnetic properties of non-aged Pu without impurities. These data indicate the absence of any ordered or disordered, static or dynamic magnetic moments in Pu at low temperatures [5, 6].

Recent progress in calculation methods allows correctly describing the ground state of pure Pu in the α-phase and the model α-phase [7, 8]. It was shown in [7] that the delicate balance between spin–orbit (SO) and exchange interactions determines the nonmagnetic ground state in pure Pu. These interactions have the magnitude close to each other in actinides and its compounds and the balance could be easily broken by crystal field of legands. Also, Söderlind [9] confirms the important role of SO and orbital polarization in formation of the nonmagnetic ground state of plutonium in the framework of model density functional theory (DFT) calculation. Impurities like Al and Ga that are used to stabilize the fcc-phase of Pu act in the same way. Several groups report the presence of the ordered magnetic moment in aged Pu–Al and Pu–Ga alloys [10–12]. The magnitude of moments is small, $\leq 10^{-3}$ μ_B ([10])—0.15 μ_B ([11, 12]), and these moments could arise due to distortion of the crystal structure near interstitial Pu atoms and vacancies.

A substantial drawback of the local (spin) density approximation (L(S)DA) is the underestimation of the orbital moment [13, 14]. As a result, the DFT in description of 4*f*- and 5*f*-metals fails, since the orbital moment in them can overcome the spin one. Taking the Coulomb repulsion U and SO interactions in full matrix rotation-invariant form into account in the LDA + U + SO method could improve the results. An achievement of this method is that the exact magnetic order does not have to be set at the start of iterations. Both the magnitude and the direction of the magnetic moment are calculated for each atom. Magnetic order and the "easy axis" direction are the result of a self-consistent interaction procedure.

In the LDA + U method [15], the energy functional $E_{\mathrm{LDA+U}}$ depends, in addition to the charge density $\rho(\mathbf{r})$, on the occupation matrix $n^{ss'}_{mm'}$ for a particular orbital for which correlation effects are taken into account (in our case, it is the 5*f* plutonium orbital). The LDA + U method in the general form nondiagonal in spin variables was defined in [16]:

$$E_{\mathrm{LDA+U}}[\rho(\mathbf{r}), \{n\}] = E_{\mathrm{LDA}}[\rho(\mathbf{r})] + E_{\mathrm{U}}[\{n\}] - E_{\mathrm{dc}}[\{n\}], \quad (1)$$

where $\rho(\mathbf{r})$ is the charge density and $E_{\mathrm{LDA}}[\rho(\mathbf{r})]$ is the standard LDA functional. The occupation matrix is defined as

$$n^{ss'}_{mm'} = -\frac{1}{\pi}\int^{E_F} \mathrm{Im} G^{ss'}_{mm'}(E)dE, \quad (2)$$

where $G^{ss'}_{mm'}(E) = \langle ms|(E - \hat{H}_{\mathrm{LDA+U}})^{-1}|m's'\rangle$ are the elements of the Green's function matrix in a local orbital basis set (*m* is the magnetic quantum number and *s* is the spin index for the correlated orbital). In

[1] The article is published in the original.

this paper, this basis set is formed of LMT-orbitals from the tight-binding LMTO method based on the atomic sphere approximation (TB–LMTO–ASA) [17]. In Eq. (1), the Coulomb interaction energy term $E_U[\{n\}]$ is a function of the occupation matrix $n^{ss'}_{mm'}$:

$$E_U[\{n\}] = \frac{1}{2}\sum_{\{m\},ss'}\{\langle m, m''|V_{ee}|m', m'''\rangle n^{ss}_{mm'}n^{s's'}_{m''m'''} - \langle m, m''|V_{ee}|m''', m'\rangle n^{ss'}_{mm'}n^{s's}_{m''m'''}\}, \quad (3)$$

where V_{ee} is the screened Coulomb interaction between correlated electrons. Finally, the last term in Eq. (1) correcting for double counting is a function of the total number of electrons in the spirit of the LDA and is a functional of the total charge density,

$$E_{dc}[\{n\}] = \frac{1}{2}UN(N-1) - \frac{1}{4}J_H N(N-2), \quad (4)$$

where $N = \mathrm{Tr}(n^{ss'}_{mm'})$ is the total number of electrons in a particular shell, and U and J_H are the screened Coulomb and Hund exchange parameters, which can be determined in the constrain LDA calculations [18, 19]. The screened Coulomb interaction matrix elements $\langle m, m''|V_{ee}|m', m''\rangle$ can be expressed in terms of the parameters U and J_H (see [15]).

The functional in Eq. (1) defines the effective single-particle Hamiltonian with an orbital-dependent potential added to the usual LDA potential:

$$\hat{H}_{LDA+U} = \hat{H}_{LDA} + \sum_{ms,m's'}|ms\rangle V^{ss'}_{mm'}\langle m's'|, \quad (5)$$

where

$$V^{ss'}_{mm'} = \delta_{ss'}\sum_{m'',m'''}\{\langle m, m''|V_{ee}|m', m'''\rangle n^{-s,-s}_{m''m'''} + (\langle m, m''|V_{ee}|m', m'''\rangle - \langle m, m''|V_{ee}|m''', m'\rangle)n^{ss}_{m''m'''}\} - (1-\delta_{ss'})\sum_{m'',m'''}\langle m, m''|V_{ee}|m''', m'\rangle n^{s's}_{m''m'''} - U\left(N-\frac{1}{2}\right) + \frac{1}{2}J_H(N-1). \quad (6)$$

In this paper, we use the LDA + U + SO method, which includes the LDA + U Hamiltonian (6), nondiagonal in spin variables, and the spin–orbit coupling term

$$\hat{H}_{LDA+U+SO} = \hat{H}_{LDA+U} + \hat{H}_{SO}, \quad \hat{H}_{SO} = \lambda\mathbf{L}\cdot\mathbf{S}, \quad (7)$$

where λ is the spin–orbit coupling parameter. In the *LS* basis, the SO coupling matrix has nonzero matrix elements that are diagonal ($(H_{SO})^{s,s}_{m',m}$) as well as off-diagonal ($(H_{SO})^{\uparrow,\downarrow}_{m',m}$ and $(H_{SO})^{\downarrow,\uparrow}_{m',m}$) in spin variables (complex spherical harmonics) [20]:

$$(H_{SO})^{\uparrow,\downarrow}_{m',m} = \frac{\lambda}{2}\sqrt{(l+m)(l-m+1)}(\delta_{m',m-1}),$$
$$(H_{SO})^{\downarrow,\uparrow}_{m',m} = \frac{\lambda}{2}\sqrt{(l+m)(l-m+1)}(\delta_{m'-1,m}), \quad (8)$$
$$(H_{SO})^{s,s}_{m',m} = \lambda ms\delta_{m',m},$$

where l, m are orbital quantum numbers and the spin index is $s = +1/2, -1/2$. The peculiarities of the LDA + U + SO method and its implementation to the problem of pure Pu and several plutonium compounds were described in detail in [7].

In this paper, four different fcc-Pu supercells are investigated: one interstitial (IS) Pu atom in a 32-atom supercell, a vacancy in an 8-atom supercell, and two 32-atom supercells with both an IS and a vacancy at minimal and large distances. Due to the presence of defects, the perfect fee structure was to be distorted, and therefore the relaxation of the crystal structure for all supercells under investigation should be taken into account. Because the LMTO method does not allow performing structure relaxation correctly, we use the classical molecular dynamics (CMD) with the modified embedded atom model (MEAM) by Baskes [21–23] as the interatomic potential. The MEAM is a many-body potential, i.e., interaction between a pair of atoms depends on the local structure (on positions of their common neighbors). The parameterization of the MEAM for pure plutonium and plutonium-gallium alloys was given in [21] and the potential is currently widely used in CMD simulations of plutonium properties and processes in Pu caused by self-irradiation [21–25].

Adding an IS or a vacancy to initial supercell makes the Pu atoms inequivalent. That is why the different types of atoms in the tables below have additional numbers (e.g., Pu1, etc). The crystal structure relaxation lowers the symmetry again, and the new Pu classes are divided into subclasses (see Table 4). All calculations of the electronic structure and magnetic properties were made using the tight-binding linear muffin-tin orbitals method with the atomic sphere approximation (the TB–LMTO–ASA computation scheme). In the LDA + U calculation scheme, the values of the direct Coulomb (U) and Hund exchange (J_H) parameters should be determined as the first step of the calculation procedure. This can be done in an *ab initio* way by constrained LDA calculations [18, 19]. In our calculations, the

Table 1. Magnetic properties calculated for the 32-atom supercell and an interstitial (IS) Pu atom. First column: the labels of nonequivalent Pu atoms. Second column: the distance between the IS and the Pu ion (Å). The next four columns: the number of equivalent Pu atoms in subclasses (n_{atoms}), calculated values for spin (S), orbital moments (L), and total moments (J). The last four columns contain partial contributions of f^6 configurations and the jj type of coupling for the $5f$ shell of the Pu ion, the effective magnetic moment, and the total number of f-electrons

	D, Å	n_{atoms}	S	L	J	f^6, %	jj, %	μ_{eff}	n_f
IS		1	0.028	0.057	0.03	98.9	99.2	0.146	6.06
Pu1	2.79	4	0.260	0.341	0.08	96.7	91.7	0.234	5.69
		2	0.065	0.059	0.01	99.8	97.8	0.061	
Pu2	4.03	4	0.216	0.310	0.09	96.3	93.2	0.256	5.79
		4	0.197	0.277	0.08	96.8	93.8	0.238	
Pu3	5.22	4	0.506	0.633	0.13	94.9	83.5	0.271	5.77
		8	0.380	0.472	0.09	96.3	87.7	0.236	
Pu4	6.96	4	0.750	1.111	0.36	85.6	75.7	0.456	5.73
		2	0.471	0.574	0.10	95.9	84.6	0.246	

Hund exchange parameter J_H was found to be $J_H = 0.48$ eV. The value of the Coulomb parameter U was set to 2.5 eV because this value provides the correct equilibrium volume of δ-Pu (see [7] for the details).

2. INTERSTITIAL PLUTONIUM ATOM IN A 32-ATOM SUPERCELL

First, the 32-atom supercell of fcc-Pu with one additional Pu atom was considered. The supercell has three coordination spheres around the defect, which is sufficient for describing relaxation of the position of neighboring atoms. The classical molecular dynamics method was used to describe distortion of the crystal structure. New positions of Pu atoms in the supercell were used in the subsequent calculation of the electronic structure. Adding one additional Pu atom lowers the symmetry of the cell. Four new inequivalent classes of plutonium belonging to four different coordination spheres around the IS arise. Moreover, the Pu atoms within each new class become inequivalent due to different local neighborhoods. To take this lowering of symmetry into account, no symmetrization was applied in our electronic structure calculation. Because no additional symmetry conditions were imposed on the electronic subsystem, the magnitude of local moments at Pu sites and their directions can be arbitrary and correspond to the minimum of the total energy.

The LDA + U + SO calculations for metallic Pu in the δ phase gave a nonmagnetic ground state with zero values of the spin S, orbital L, and total J moments [7, 8].

Our calculation for the 32-atom supercell with one IS shows that small local magnetic moments develop at the Pu sites. The local moment magnitude depends on the distance between the center of distortion (IS) and the corresponding Pu site. We argue that this is because of a violation of the balance between SO and exchange interactions due to the crystal structure relaxation. The results are presented in Table 1. The partial contributions of the f^6 configuration and the jj-type of coupling to the final state can be calculated in the following way. The total moment value is the same in both coupling schemes (jj or LS): $J = 0$ for f^6 and $J = 5/2$ for f^5. If there is a mixed state $(1 - x)f^6 + xf^5$, then x can be defined as $x = J/2.5$. The spin S and orbital L moment values for the f^6 configuration are equal to zero in the jj coupling scheme and $S = 3$, $L = 3$ in the LS coupling scheme. For the f^5 configuration, they are $S = 5/14 \approx 0.36$ and $L = 20/7 \approx 2.86$ in the jj coupling scheme, and $S = 5/2$ and $L = 5$ in the LS coupling scheme. We can define a mixed coupling scheme with a contribution of the jj coupling equal to y and of the LS coupling equal to $1 - y$. In the final state, the calculated values of orbital and spin moments are

$$L = x(2.86y + 5(1-y)) + (1-x)(0\cdot y + 3(1-y)), \quad (9)$$

$$S = x(0.36y + 2.5(1-y)) + (1-x)(0\cdot y + 3(1-y)). \quad (10)$$

These formulas allow determining the value of the coefficient y. An effective paramagnetic moment obtained from susceptibility measurements using the Curie-Weiss law can be calculated as

$$\mu_{\text{eff}} = g\sqrt{J(J+1)}\mu_B. \quad (11)$$

The problem is to define the Lande g-factor that can be calculated for pure f^5 and f^6 configurations in the LS or jj coupling schemes. For the f^6 configuration, the total moment $J = 0$, and we therefore need to calculate the g-factor for the f^5 configuration only. For

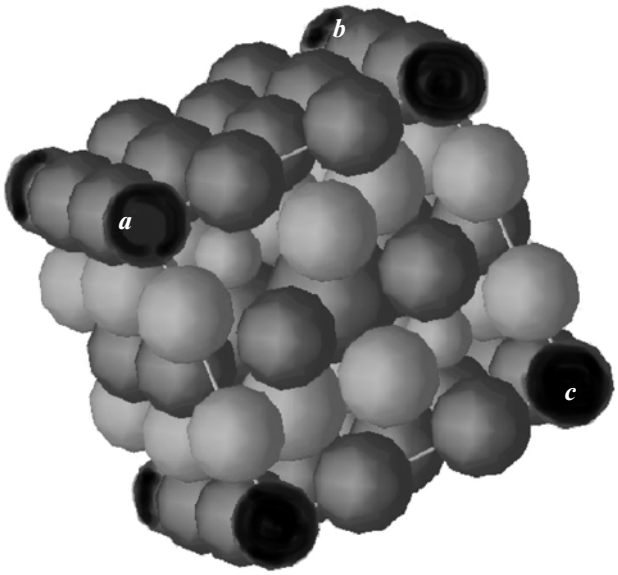

Fig. 1. Noncollinear order obtained for the 32-atom supercell with an IS. Black spheres at the corners denote the IS. Light and dark gray spheres are Pu atoms with oppositely directed total moments. The radii of the spheres are proportional to the magnitude of the corresponding magnetic moments.

the ground state of the f^5 configuration in the *jj* coupling scheme, the Lande factor is $g_{jj} = 6/7 \approx 0.86$. In the *LS* coupling scheme, its value is $g_{LS} = 2/7 \approx 0.29$. Because the latter value is nearly three times larger than the former, g_{jj} and g_{LS} can give only upper and lower limits of the *g*-factor in the case of intermediate coupling. We can calculate the weighted value of the effective moment using the relative weights of *LS*- and *jj*-couplings obtained from Eqs. (9), (10), and (11).

The magnetic order of Pu ions is set arbitrarily at the beginning of the iteration process. Final directions of local moments are calculated in accordance with the minimum of the total energy at the end of the self-consistence loop. Because the long-range order is set up in the chosen calculation method, some ferrimagnetic order arouse as an artifact. This order resembles the antiferromagnetic (AFM) one of the A-type. In Fig. 1, the resulting directions of the total moment are shown with red and green colors. Pu atoms positioned in the first coordination sphere to the IS as well as the IS itself have the smallest magnetic moments. They do not differ significantly from those in pure δ-Pu, which is nonmagnetic. The values of local moments increase as the distance between the IS and the corresponding site increases. The largest total moment develops for the Pu4 ion positioned in the center of the supercell (the large sphere in Fig. 1). This ion has the largest distance to the IS. The average value of the effective moment for an IS Pu atom in the 32-atom supercell is $\mu_{\text{eff}} \sim 0.26\mu_B$. The numbers of *f*-electrons (see Table 1, last column) differ from those calculated for nondistorted fcc-Pu (which has 5.74 *f*-electrons), but not significantly except the case of the interstitial atom. The later has the largest occupation number in all considered structures (see the tables below). The large number of *f*-electrons (close to 6) obtained in the present calculation disagrees with previous experimental and theoretical estimations that give 5.1–5.2 electrons [26]. Such a difference between theoretical results originates from dissimiliar band structure calculation methods. Since the TB–LMTO–ASA scheme uses artificially large overlapping atomic spheres, these numbers should be only used to compare different classes of plutonium atoms with each other. We have verified our results and run several calculations with different radii of Pu atoms, filling empty space in the primitive cell with empty spheres (pseudoatoms without core states). A distorted supercell always becomes magnetic with the same order. The magnitude of local magnetic moments depends slightly on the atomic radius. It increases as the radius increases. For simplicity, we chose the same radii 3.41 a.u. for all Pu atoms, in order to be able to compare their magnetic moments. Artificial overlapping of atomic spheres in all the supercells considered never exceeds 13%, which is the critical TB–LMTO–ASA value.

3. VACANCY IN AN 8-ATOM SUPERCELL

Another type of defects appearing in Pu during the first several years of storage is vacancy. Just the vacancies mostly survive and affect thermodynamic and mechanical properties of Pu [27, 28].

A small supercell consisting of eight Pu atoms was considered. One Pu atom was removed from its position in the supercell and after relaxation of the crystal structure this empty space was artificially filled with an empty sphere. Unfortunately, the 8-atom supercell is not sufficient for correct describing the crystal structure relaxation within the MEAM. Shifts of Pu atoms were obtained to be negligible. Nevertheless, removing one atom from the supercell lowers the symmetry of crystal, because the local neighborhood of plutonium atoms becomes different. We note that this suffices to induce local moments on Pu sites. In contrast to the IS action, the vacancy much stronger affects the Pu1 that form the first coordination sphere (Table 2). Magnetic moments of Pu2 atoms that belong to the 2nd coordination sphere are smaller.

The average value of the effective magnetic moment in the supercell with a vacancy is about $0.28\mu_B$. In contrast to the case of the IS in a 32-atom supercell, the resulting magnetic order is an analogue of a C-type AFM (see Fig. 2).

These results prove that both types of defects induce local magnetic moment on Pu atoms due to distortion of the fee structure or even lowering the symmetry. Different types of defects affect magnetism in Pu in different ways: an IS induces larger magnetic moments on atoms at large distance, whereas a vacancy mostly affects its nearest neighbors. Different types of defects also result in different types of AFM order. The simul-

Table 2. Magnetic properties of Pu ions calculated for the 8-atom supercell with one vacancy. Second column shows the distance between the vacancy and the Pu ion (Å). See also the caption to Table 1.

	D, Å	n_{atoms}	S	L	J	f^6, %	jj, %	μ_{eff}	n_f
Pu1	3.27	2	0.651	0.817	0.166	93.4	78.7	0.298	5.71
		2	0.518	0.656	0.138	94.5	83.1	0.283	
		2	0.515	0.652	0.137	94.5	83.3	0.283	
Pu2	4.63	1	0.356	0.449	0.094	96.3	88.5	0.243	5.70

taneous effect of an IS and a vacancy could also give rise to the local moments and lead to a more complicated pattern of the Pu–ion magnetic order.

4. VACANCY AND INTERSTITIAL PLUTONIUM AT THE MINIMAL DISTANCE

Because an IS and a vacancy affect the magnetism in Pu in different ways, we can expect that their simultaneous influence could also give rise to a local moment and produce some complicated magnetic pattern.

As the first step, a 32-atom supercell with an IS and a vacancy at the minimal distance was investigated. Relaxation of the supercell was made using molecular dynamics within the MEAM. Both the removal of one Pu atom from its site and relaxation lower the symmetry of the supercell, and one class of Pu is divided into 11 classes. Six of them have two subclasses (see Table 3). Small local moments also develop at Pu sites of the relaxed supercell. The magnitude of moments and other results of an LDA + U + SO calculation are presented in Table 3. Two different values of moments for one type of Pu atoms occur because of lowering the supercell symmetry due to orbital polarization. The mutual action of the IS and the vacancy decreases the dispersion of magnitudes on different sites. The average value of the effective moment at a Pu atom is $0.18\mu_B$.

Three types of Pu atoms, Pu10, Pu1, and Pu3, have the largest magnetic moments, $0.261\mu_B$, $0.259\mu_B$, and $0.252\mu_B$ respectively. Atoms of type Pu1 and Pu3 are the nearest to the vacancy (except the IS) and hence

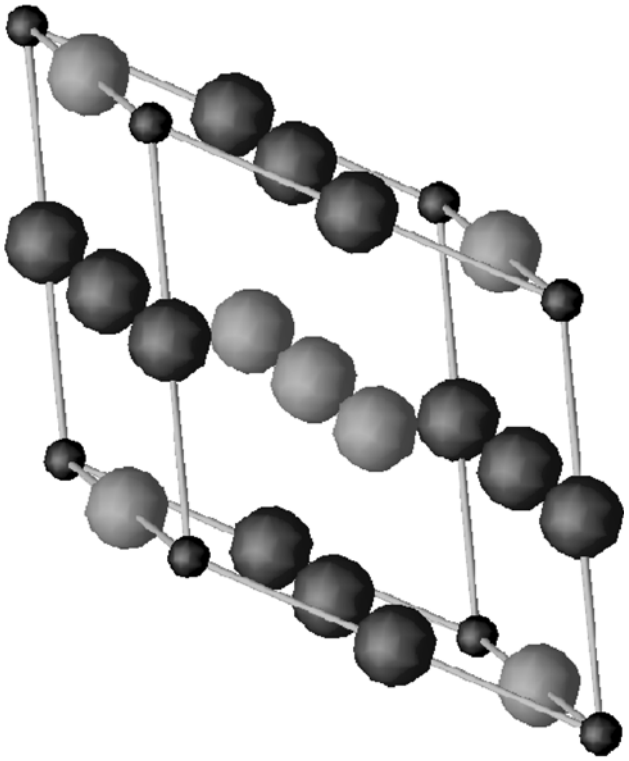

Fig. 2. Noncollinear order obtained for the 8-atom supercell with a vacancy. The vacancy is shown as black spheres. Light and dark gray spheres. Light and dark gray spheres are Pu atoms with oppositely directed total moments. The radii of spheres are proportional to the magnitude of the corresponding magnetic moment.

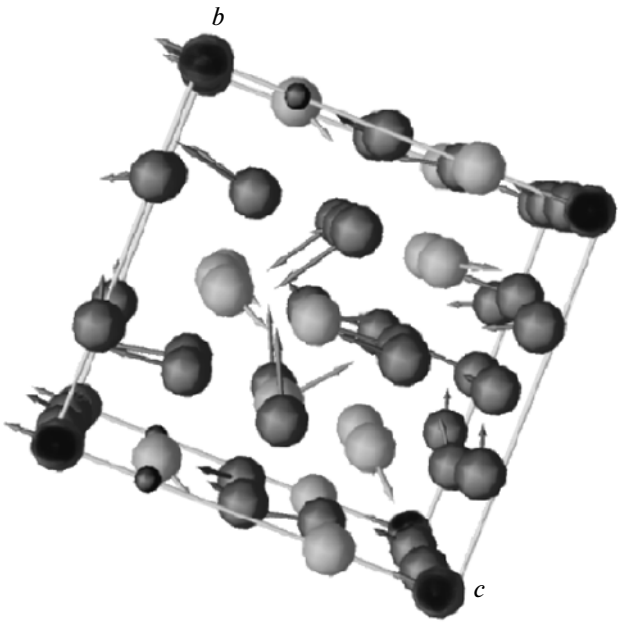

Fig. 3. Ferrimagnetic order obtained for the 32-atom supercell with an IS and a vacancy at the minimal distance. Small black spheres denote the vacancy, and large black spheres at the corners, the IS. Light and dark gray spheres are Pu atoms with opposite signs of the z-component of the magnetic moment. The length of arrows is proportional to the magnitude of the corresponding effective magnetic moment.

Table 3. Magnetic properties of Pu ions calculated for the 32-atom supercell with one vacancy and an IS at the minimal distance. See also caption to Table 1

	D, Å	n_{atoms}	S	L	J	f^6, %	jj, %	μ_{eff}	n_f
IS		1	0.058	0.086	0.029	98.9	98.2	0.145	6.1
Pu1	4.02	2	0.250	0.348	0.097	96.1	92.0	0.259	5.61
		2	0.195	0.267	0.073	97.1	93.8	0.225	
Pu2	2.70	1	0.009	0.015	0.006	99.8	99.7	0.064	6.22
Pu3	5.10	2	0.485	0.583	0.098	96.1	84.1	0.237	5.71
		2	0.532	0.645	0.113	95.5	82.6	0.252	
Pu4	6.91	2	0.230	0.313	0.083	96.7	92.7	0.239	5.75
		2	0.021	0.038	0.017	99.3	99.4	0.111	
Pu5	4.09	2	0.165	0.212	0.047	98.1	94.7	0.180	5.71
		2	0.122	0.155	0.033	98.7	96.1	0.153	
Pu6	2.85	2	0.057	0.081	0.024	99.1	98.2	0.132	5.78
		2	0.088	0.117	0.029	98.8	97.2	0.145	
Pu7	5.18	2	0.123	0.156	0.034	98.7	96.1	0.154	5.75
Pu8	6.91	1	0.069	0.077	0.008	99.7	97.7	0.074	5.75
Pu9	5.35	2	0.220	0.277	0.057	97.7	92.9	0.196	5.77
Pu10	6.99	2	0.343	0.448	0.105	95.8	88.9	0.261	5.78
Pu11	5.24	2	0.069	0.095	0.027	98.9	97.8	0.140	5.79
		2	0.150	0.199	0.049	98.0	95.2	0.186	

have the largest magnetic moments in agreement with the results of our previous calculation for the vacancy in an 8-atom supercell (Sec. 3). Pu6 atoms belong to the first coordination sphere of the vacancy, but have much smaller moments, about $0.14\mu_B$. These atoms are positioned in the first coordination sphere of the IS and, in agreement with our results for one IS in the 32-atom supercell, the IS suppresses magnetism on Pu6 atoms. Finally, Pu10 has a sizeable magnetic moment, although it is smaller than that at the Pu atom in the center of the 32-atom supercell with a single IS. This could be explained by the action of the vacancy that induces large local moments near itself and suppresses the magnetism on distant atoms.

The simultaneous effect of an IS and a vacancy results in a more complicated canted AFM pattern, which could not be identified with any standard type. The calculated canted AFM order is presented in Fig. 3.

5. VACANCY AND INTERSTITIAL PLUTONIUM AT LARGE DISTANCE

Finally, we made the same calculation for a 32-atom supercell containing an IS and a vacancy at a large distance. As in the previous cases, the crystal structure relaxation was made within the MEAM before the band structure calculation. The considered defects also lower the symmetry and 17 new Pu classes arise. The values of moments and the contribution of coupling types and electronic configurations are presented in Table 4.

As in our calculation for the IS and the vacancy at the minimal distance, local moments develop at all Pu atoms. The magnitude of the moments depends on the distances to both the IS and the vacancy. Incommensurate magnetic order with strong noncollinearity was obtained for this type of defect positions (see Fig. 4). The mechanism of the formation of magnetic moments was described above. The average magnetic moment on Pu is $0.179\mu_B$.

6. CONCLUSIONS

Band structure calculations have been run for four supercells containing an IS, a vacancy, and both the IS and vacancy at small and large distances. For the supercell with one IS, ferrimagnetic order close to the A-type AFM was obtained. The magnitudes of local moments are $0.06–0.46\mu_B$ and the average moment is $0.26\mu_B$. Atoms at the longest distance from the IS have the largest magnetic moments. Ferrimagnetic order close to the C-type AFM was obtained for the 8-atom supercell with a vacancy. This type of defect induces the largest moment on Pu atoms in first coordination sphere. Magnetic moments obtained in the 32-atom supercell with both the IS and vacancy have a smaller dispersion, $(0.1–0.3)\mu_B$, and a smaller averaged moment, about $0.18\mu_B$. Simultaneous action of these defects results in

Table 4. Magnetic properties calculated for the 32-atom supercell with one vacancy and the IS at a large distance. See also caption to Table 1

	D, Å	n_{atoms}	S	L	J	f^6, %	jj, %	μ_{eff}	n_f
IS		1	0.052	0.083	0.032	98.7	98.4	0.153	6.12
Pu1	4.26	4	0.144	0.176	0.032	98.7	95.4	0.149	5.70
Pu2	2.79	2	0.103	0.141	0.038	98.5	96.7	0.164	5.78
Pu3	5.01	1	0.235	0.333	0.098	96.0	92.6	0.261	5.73
Pu4	6.67	2	0.152	0.188	0.035	98.6	95.1	0.157	5.72
Pu5	3.77	4	0.268	0.361	0.093	96.3	91.4	0.250	5.70
Pu6	3.11	1	0.065	0.091	0.025	99.0	97.9	0.136	5.73
Pu7	5.25	2	0.031	0.039	0.007	99.7	99.0	0.072	5.74
Pu8	7.12	1	0.173	0.219	0.046	98.2	94.4	0.178	5.71
Pu9	2.63	1	0.077	0.128	0.051	98.0	97.7	0.194	6.01
Pu10	4.90	2	0.226	0.276	0.050	98.0	92.7	0.182	5.75
Pu11	6.83	1	0.169	0.276	0.107	95.7	94.8	0.280	5.73
Pu12	2.79	2	0.020	0.031	0.012	99.5	99.4	0.093	5.82
Pu13	4.87	2	0.139	0.181	0.042	98.3	95.5	0.172	5.78
Pu14	7.29	2	0.073	0.131	0.058	97.7	97.8	0.208	5.75
Pu15	5.23	2	0.239	0.303	0.065	97.4	92.3	0.208	5.77
Pu16	5.42	1	0.164	0.228	0.064	97.5	94.8	0.212	5.78
Pu17	5.02	1	0.245	0.312	0.068	97.3	92.1	0.213	5.79

incommensurate magnetic order with strong noncollinearity. Nevertheless, the long-range order obtained in this work should be regarded as an artifact of the computation method. Our results indicate that short-range order could appear due to defects in fcc Pu, and the type of such order depends strongly on the distance to the corresponding defect. The implementation of the LDA + DMFT method is necessary for a more accurate description of the magnitudes of local moments in the paramagnetic phase of Pu.

The results of calculations explain the presence of magnetic moment in aged Pu samples and agree well with experimental data [6, 11, 12].

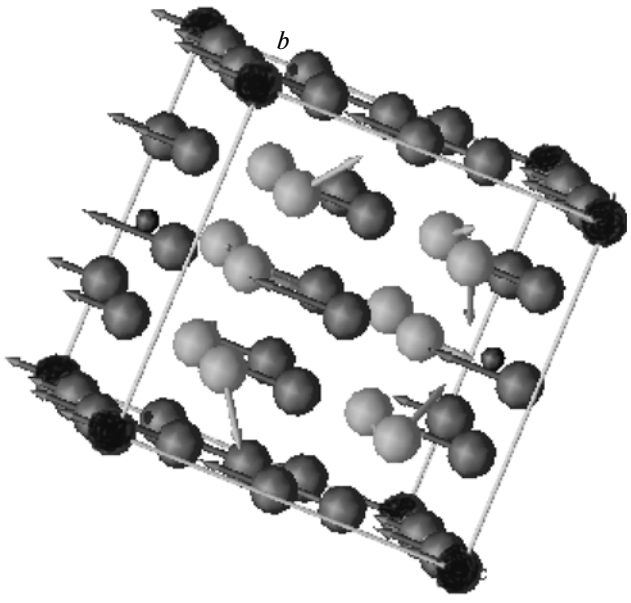

Fig. 4. Ferrimagnetic order obtained for the 32-atom supercell with an IS and a vacancy at a large distance. See also caption to Fig. 3.

ACKNOWLEDGMENTS

The study was supported by the Russian Foundation for Basic Research (project nos. 13-02-00050 and 12-02-91371-CT_a), Ural Branch of the Russian Academy of Sciences (project no. 13-2-006-NC), the Ministry of Education and Science of the Russian Federation (project nos. 14.A18.21.0076, 12.740.11.0026, and 14.A18.21.0737), the fund of the president of the Russian Federation (grant no. NSh-6172.2012.2), Program of the Russian Academy of Sciences Presidium "Quantum Microphysics of Condensed Matter" (12-П-2-1017, 12-CD-2), and by contract LANL–RFNC-VNIITF no. 04783-000-99-35 TO 014.

REFERENCES

1. S. Y. Savrasov and G. Kotliar, Phys. Rev. Lett. **84**, 3670 (2000).
2. *Plutonium—A General Survey*, Ed. by K. H. Lieser (Chemie, Berlin, 1974).

3. J. Bouchet, B. Siberchicot, F. Jollet, and A. Pasturel, J. Phys.: Condens. Matter **12**, 1723 (2000).
4. P. Söderlind, A. L. Landa, and B. Sadigh, Phys. Rev. B: Condens. Matter **66**, 205109 (2002).
5. J. C. Lashley, A. Lawson, R. J. McQueeney, and G. H. Lander, Phys. Rev. B: Condens. Matter **72**, 054416 (2005).
6. R. H. Heffner, G. D. Morris, M. J. Fluss, B. Chung, S. McCall, D. E. MacLaughlin, L. Shu, K. Ohishi, E. D. Bauer, J. L. Sarrao, W. Higemoto, and T. U. Ito, Phys. Rev. B: Condens. Matter **73**, 094453 (2005).
7. A. O. Shorikov, A. V. Lukoyanov, M. A. Korotin, and V. I. Anisimov, Phys. Rev. B: Condens. Matter **72**, 024458 (2005).
8. A. B. Shick, V. Drchal, and L. Havela, Europhys. Lett. **69**, 588 (2005).
9. P. Söderlind, Phys. Rev. B: Condens. Matter **77**, 085101 (2008).
10. R. H. Heffner, K. Ohishia, M. J. Fluss, G. D. Morris, D. E. MacLaughlin, L. Shu, B. W. Chung, S. K. McCall, E. D. Bauer, J. L. Sarrao, T. U. Ito, and W. Higemoto, J. Alloys Compd. **444–445**, 80 (2007).
11. S. V. Verkhovkii, V. E. Arkhipov, Yu. N. Zuev, Yu. V. Piskunov, K. N. Mikhalev, A. V. Korolev, I. L. Svyatov, A. V. Pogudin, V. V. Ogloblichev, and A. L. Buzlukov, JETP Lett. **82** (3), 139 (2005).
12. S. Verkhovskii, Yu. Piskunov, K. Mikhalev, A. Buzlukov, V. Arkhipov, Yu. Zouev, A. Korolev, S. Lekomtsev, I. Svyatov, A. Pogudin, and V. Ogloblichev, J. Alloys Compd. **444–445**, 288 (2007).
13. M. Singh, J. Callaway, and C. S. Wang, Phys. Rev. B: Solid State **14**, 1214 (1976).
14. C. T. Chen, Y. U. Idzerda, H.-J. Lin, N. V. Smith, G. Meigs, E. Chaban, G. H. Ho, E. Pellegrin, and F. Sette, Phys. Rev. Lett. **75**, 152 (1995).
15. For the review, see *Strong Coulomb Correlations in Electronic Structure Calculations: Beyond the Local Density Approximation*, Ed. by V. I. Anisimov (Gordon and Breach, Amsterdam, The Netherlands, 2000); V. I. Anisimov, F. Aryasetiawan, and A. I. Lichtenstein, J. Phys.: Condens. Matter **9**, 767 (1997).
16. I. V. Solovyev, A. I. Liechtenstein, and K. Terakura, Phys. Rev. Lett. **80**, 5758 (1998).
17. O. K. Andersen, Phys. Rev. B: Solid State **12**, 3060 (1975); O. Gunnarsson, O. Jepsen, and O. K. Andersen, Phys. Rev. **27**, 7144 (1983).
18. O. Gunnarsson, O. K. Andersen, O. Jepsen, and J. Zaanen, Phys. Rev. B: Condens. Matter **39**, 1708 (1989).
19. V. I. Anisimov and O. Gunnarsson, Phys. Rev. B: Condens. Matter **43**, 7570 (1991).
20. L. D. Landau and E. M. Lifshitz, *Course of Theoretical Physics*, Volume 3: *Quantum Mechanics: Non-Relativistic Theory* (Nauka, Moscow, 1974; Butterworth–Heinemann, Oxford, 1981), p. 115.
21. M. I. Baskes, A. C. Lawson, and S. M. Valone, Phys. Rev. B: Condens. Matter **72**, 014129 (2005).
22. S. M. Valone, M. I. Baskes, and R. L. Martin, Phys. Rev. B: Condens. Matter **73**, 214209 (2006).
23. M. I. Baskes, S. Y. Hu, S. M. Valone, G. F. Wang, and A. C. Lawson, J. Comput.-Aided Mater. Des. **14**, 379 (2007).
24. V. V. Dremov, F. A. Sapozhnikov, S. I. Samarin, D. G. Modestov, and N. E. Chizhkova, J. Alloys Compd. **444–445**, 197 (2007).
25. V. Dremov, P. Sapozhnikov, A. Kutepov, V. Anisimov, M. Korotin, A. Shorikov, D. L. Preston, and M. A. Zocher, Phys. Rev. B: Condens. Matter **77**, 224306 (2008).
26. J. G. Tobin, P. Söderlind, A. Landa, K. T. Moore, A. J. Schwartz, B. W. Chung, M. A. Wall, J. M. Wills, R. G. Haire, and A. L. Kutepov, J. Phys.: Condens. Matter **20**, 125204 (2008); T. Björkman and O. Eriksson, Phys. Rev. B: Condens. Matter **78**, 245101 (2008).
27. V. V. Dremov, A. V. Karavaev, S. I. Samarin, F. A. Sapozhnikov, M. A. Zocher, and D. L. Preston, J. Nucl. Mater. **385**, 79 (2008).
28. V. V. Dremov, A. V. Karavaev, F. A. Sapozhnikov, M. A. Vorobyova, D. L. Preston, and M. A. Zocher, J. Nucl. Mater. **414**, 471 (2011).